IEEE Access
Multidisciplinary | Rapid Review | Open Access Journal

Received September 12, 2019, accepted October 3, 2019, date of publication October 14, 2019, date of current version October 25, 2019.

Digital Object Identifier 10.1109/ACCESS.2019.2947194

A Generative Adversarial Network-Based Intelligent Fault Diagnosis Method for Rotating Machinery Under Small Sample Size Conditions

YU DING, LIANG MA, JIAN MA, CHAO WANG, AND CHEN LU
School of Reliability and Systems Engineering, Beihang University, Beijing 100191, China
Science and Technology on Reliability and Environmental Engineering Laboratory, Beijing 100191, China

Corresponding author: Chen Lu (luchen@buaa.edu.cn)

This work was supported in part by the National Natural Science Foundation of China under Grant 61973011, Grant 61803013, and Grant 61903015, in part by the Fundamental Research Funds for the Central Universities under Grant ZG140S1993, in part by the National key Laboratory of Science and Technology on Reliability and Environmental Engineering under Grant 6142004180501 and Grant WDZC2019601A304, and in part by the China Postdoctoral Science Foundation under Grant 2019M650438.

ABSTRACT Rotating machinery plays a key role in mechanical equipment, and the fault diagnosis of rotating machinery is a popular research topic. To overcome the dependency on expert knowledge regarding conventional time-frequency analysis diagnosis methods, machine learning (ML) and artificial intelligence (AI)-based methods are commonly studied. Although these methods can achieve high-accuracy diagnosis results, they are based on a large number of training samples. A generative adversarial network (GAN) is an algorithm with the capability of generating realistic samples that are similar to the real samples, and it can be applied to solve fault diagnosis problems with insufficient training data, which is called the small sample size condition in this study. However, a single-GAN model cannot achieve a good diagnostic result. To achieve adaptive feature extraction and high diagnosis accuracy, this study proposes an intelligent fault diagnosis method for rotating machinery based on GANs under small sample size conditions. The effectiveness and performance of the proposed method are validated using rolling bearing and gearbox datasets. In these datasets, only 10% and 20% of the samples are selected as the training data. Samples associated with different health conditions and various working conditions are included in the datasets. Compared with those of other diagnosis methods, the high-accuracy and low-volatility diagnosis results indicate that the proposed method can stably distinguish fault modes under different working conditions in an adaptive way, even though few training samples are available.

INDEX TERMS Fault diagnosis, rotating machinery, generative adversarial network, small sample size conditions.

I. INTRODUCTION

In industrial production, rotating machinery is an indispensable and important general-purpose component in mechanical equipment and plays a crucial role in the operation of such equipment. The reliability of rotating machinery is challenged by poor working environments that include heavy loads and variable working conditions. Moreover, the safe operation of mechanical equipment is a core requirement in the industrial production process, and equipment failure may result in serious economic losses or even catastrophic accidents. Therefore, it is necessary to monitor and diagnose the faults of rotating machinery, locate the faults in a timely manner, and support the corresponding maintenance decisions.

There have been many studies of the fault diagnosis of rotating machinery. The conventional diagnosis methods are mainly based on vibration analysis and signal processing and use time-frequency analysis and other techniques to extract fault features from the vibration signals collected by the sensors and diagnose the fault modes. Empirical mode decomposition (EMD), which is a time-frequency analysis technique, is widely used in rotating machinery diagnosis. Studies by Loutridis [1] and Junsheng *et al.* [2] extracted the fault features from the vibration signals collected from gears and bearings, classified the fault modes and achieved good results. In addition, as classical time-frequency analysis

The associate editor coordinating the review of this manuscript and approving it for publication was Vincenzo Piuri.

methods, wavelet package transform (WPT) [3] and local mean decomposition (LMD) [4] have been fully studied for diagnosis. However, conventional diagnosis methods based on signal processing techniques often rely on expert knowledge in vibration analysis, fault diagnosis and other fields, which limits the broad application of such methods. With the development of machine learning (ML) and artificial intelligence (AI), AI-based methods have become increasingly used to adaptively mine the fault-related information from rotating machinery operating data in a data-driven way to automatically diagnose fault modes. Support vector machines (SVMs) have the capability of nonlinear multilabel classification and are used in tasks related to the diagnosis of rolling bearings [5], [6] and gears [7]. Artificial neural networks (ANNs) [7], [9], [10] simulate the biological nervous system based on the connections among artificial neurons simulated by activation functions considering the relevant weights and biases. In addition, ANNs can extract and combine nonlinear features and perform classification or regression tasks, so they can be used in the fault diagnosis of rotating machinery based on adaptive feature extraction from vibration signals. Due to the structure of deep neural networks (DNNs) and number of hidden neurons, DNNs are capable of obtaining nonlinear representations of data. They not only achieve results than conventional methods in the fields of image classification [11] and natural language processing [12] but also display excellent performance in fault diagnosis tasks. Lu *et al.* [13] proposed a diagnosis method based on the stacked denoising autoencoder, and it achieved high accuracy in the diagnosis of rolling bearings. Guo *et al.* [14] used a convolutional neural network (CNN) to extract features from the vibration signals of bearings and combine these features in a layer-by-layer method to adaptively diagnose the fault modes. Yu *et al.* [15] performed feature extraction based on the time-domain vibration signals of rotating machinery for fault diagnosis with long short-term memory (LSTM) neural networks. The fault diagnosis methods above based on ML and deep learning have a common drawback: they require a large amount of training data to automatically learn the intrinsic patterns of normal and fault data. However, in practice, 1) it is difficult to collect real operating data corresponding to different health conditions due to the low frequency of fault occurrences [16], 2) the cost and risk of fault injections to rotating machinery is very high, and such experiments may injure researchers and destroy property [17], and 3) even if large amounts of real data are available, it is costly to label these data [18], and it is generally not easy to obtain enough high-quality labeled data for model training. Hence, it is urgently needed to develop a fault diagnosis method that can achieve high-accuracy results with only a few samples for training.

A Generative adversarial networks (GAN) is a ML algorithm with the capability of generating samples in an unsupervised way. GAN was proposed by Goodfellow *et al.* [19] and can adaptively learn samples to construct a mapping from a prior random noise distribution to the intrinsic distribution hidden in real samples based on the adversarial training between the generator and discriminator. When the generator and discriminator are both well trained, the generator can output generated samples that are very similar to the real samples with random noise as the input data. The vanilla GAN and its variants, including DC-GAN [20], AC-GAN [21] and WGAN [22], etc. have achieved good generating performance on some large-scale image datasets, such as ImageNet. Because the training process of a GAN does not require a large amount of labeled data, these networks can be applied in fault diagnosis tasks with insufficient training data, which is called the small sample size condition in this study. Lee *et al.* [23] applied a GAN based method instead of other conventional resampling methods to augment an imbalanced dataset for an induction motor. Compared with other resampling methods, the GAN-based method generated more realistic samples, which increased the fault diagnosis accuracy in contrast to using an imbalanced dataset. However, this method only used the GAN for data augmentation, so the quality of the generated samples greatly influenced the accuracy of fault diagnosis. Wang *et al.* [24] proposed a fault diagnosis method based on a stacked denoising autoencoder and generative adversarial network (SDAE-GAN), which not only outputted a 0/1 flag but also the category labels of samples. This approach enables the discriminator to determine the fault mode of the sample and whether the input data come from the real data distribution. However, the difficulty of learning several distributions simultaneously is very high. According to a case study in that paper, the SDAE-GAN-based method achieved an accuracy of 90% in a 5-category fault diagnosis of a planetary gearbox, and the training set contained 500 real samples. A fault diagnosis model with only a single GAN will struggle to learn the distributions of several health conditions simultaneously with high accuracy.

These problems can be summarized into two conclusions. 1) The existing AI-based fault diagnosis methods often rely on a large amount of training data, which is practically difficult to obtain for rotating machinery. 2) The GAN-based method is a solution to the problem of fault diagnosis under the small sample size condition, but a single-GAN model may not produce a high-accuracy result. To solve these problems, this study proposes a fault diagnosis method for rotating machinery based on an ensemble GAN method. The proposed method uses multiple GANs to learn the data distribution of each health condition and then uses a semi-supervised method to enhance the feature extraction capability of the discriminator of each GAN. A multicategory fault diagnosis task is finally completed by integrating all the enhanced discriminators corresponding to the health conditions. The specific implementation process is as follows. 1) Each GAN is trained by adversarial training. During this process, the discriminators are pretrained in an unsupervised way to determine whether the input sample comes from the learned distribution. 2) The discriminators are enhanced in a semi-supervised way to improve the determination capability using the supervised training set chosen from the original small sample size

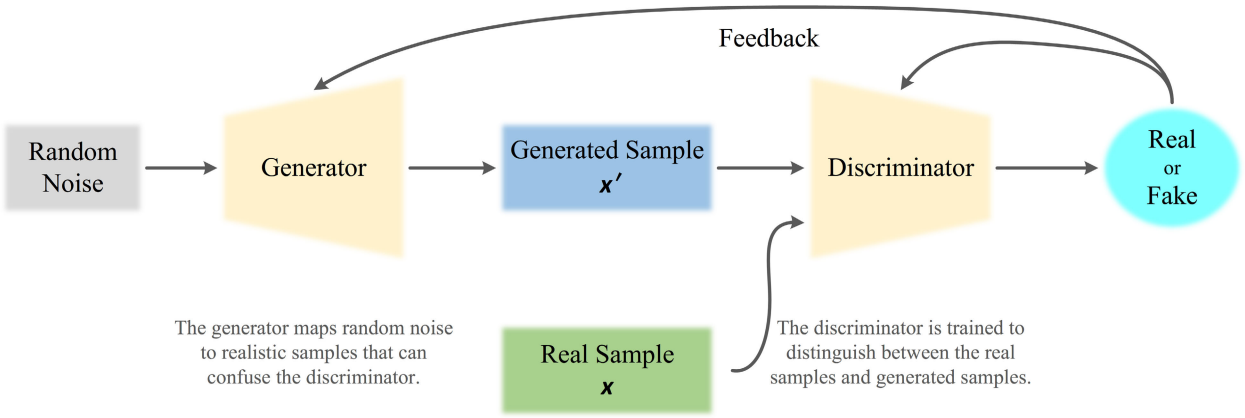

FIGURE 1. The fundamental principle of a GAN.

training set. 3) All enhanced discriminators are integrated. When a sample is obtained, it is fed into the ensemble model, and the discriminator that outputs the largest value corresponds to the predicted health condition. Compared with conventional AI-based methods, the proposed method achieves a high-accuracy diagnosis result under the small sample size condition, which overcomes the dependency on a large amount of training data. Compared to multicategory classification with a single GAN, the proposed method uses an ensemble strategy that controls each GAN to learn the relevant data distributions. Thus, the learned distributions match the real distributions, and the diagnosis accuracy is high. Moreover, the proposed discriminating ability enhancement method (DAEM) is employed for the discriminators, which further improves the performance of the diagnosis model. The main contributions of the proposed methods are as follow:

(1) Different from the idea of using data augmentation methods or resampling methods to expand the number of training samples, the proposed method can map the relationship between the corresponding measured signals and the different health conditions of the rotating machinery with only a small number of samples.

(2) The proposed method can eliminate the interaction between the intrinsic distributions of different fault modes in the training process. Thus, compared with the single-GAN based fault diagnosis method, the proposed method has stronger generalization ability.

The remainder of this paper is organized as follows. Section 2 introduces the structure of the GAN and the adversarial training method. Section 3 describes the ensemble GAN-based method proposed in this study, including the adversarial training, DAEM and ensemble diagnosis methods. Section 4 uses rolling bearing and gearbox datasets to validate the effectiveness and performance of the proposed method separately. The conclusions are drawn in section 5.

II. A BRIEF INTRODUCTION TO THE GAN

A GAN is composed of one generator and one discriminator. Inspired by binomial zero-sum game theory, the goal of training a GAN is for the generator and discriminator to reach Nash equilibrium. Any differentiable function that can be optimized using gradient-based methods can be selected as the generator and discriminator in a GAN. x_r represents the real sample, and z represents the random noise vector, such as Gaussian random noise. The goal of the generator is to capture the potential distribution hidden in real samples taking z as input. Thus, the generator outputs a "fake" sample x_f that is as similar as possible to x_r to confuse the discriminator. Moreover, the goal of discriminator is to distinguish x_f and x_r and identify the real samples and generated samples. Because the goals of the generator and discriminator are contradictive, the two parts of a GAN are in competition and become gradually stronger during training. As long as the GAN is well trained, the distribution of generated samples will match the distribution of real samples, and the discriminator will struggle to tell the difference between x_f and x_r. Because the output of the discriminator is the probability that the sample is a true/generated sample, the discriminator eventually becomes "confused" and predicts 0.5 for both the real and generated samples. From another perspective, since a GAN can capture the distribution of real samples, the discriminator can differentiate between the training samples and other samples. This capability of a GAN inspired us to design a novel fault diagnosis method under the condition of a small sample.

The fundamental principle of a GAN is shown in Fig. 1. The nonlinear functions approximated by the generator and discriminator are denoted as $D(\cdot)$ and $G(\cdot)$, respectively. The distribution of the real samples and random noise are denoted as P_{data} and P_n, respectively. Because the training goals of the generator and discriminator are different, the objective functions are defined separately. The objective functions of and are defined as (1) and (2), respectively.

$$\min_G \left\{ L_G(D, G) = E_{z\sim P_n}\left[\log\left(1 - D\left(G\left(z\right)\right)\right)\right]\right\} \tag{1}$$

$$\max_D \{L_D(D, G) = E_{x\sim P_{data}}\left[\log D\left(x\right)\right] + E_{z\sim P_n}\left[\log\left(1 - D\left(G\left(z\right)\right)\right)\right]\} \tag{2}$$

In the equations above, $L_G(D, G)$ and $L_D(D, G)$ are the objective functions of the generator and discriminator, respectively. $z \sim P_n$ indicates that the noise vector is from the distribution P_n. Additionally, $x \sim P_{data}$ suggests that the input sample is from the distribution P_{data}. $G(\cdot)$ and $D(\cdot)$ are the output values of the generator and discriminator, respectively.

Since the training process of a GAN is a game between the generator and the discriminator, the two parts of a GAN are alternately trained. Furthermore, (1) indicates that during the training process of the generator, no real samples are needed. Therefore, the first part in (2), $E_{x\sim P_{data}}\left[\log D(x)\right]$, is redundant and can be added to (1) without affecting the training process of the generator. Thus, (1) and (2) can be integrated into a single objective function for the overall training process of the GAN, and the integrated function is shown in (3).

$$\min_G \max_D \{L_D(D, G) = E_{x\sim P_{data}}\left[\log D(x)\right] + E_{z\sim P_n}\left[\log\left(1 - D(G(z))\right)\right]\} \quad (3)$$

During the adversarial training process, the generator and the discriminator are trained by the mini-batch gradient descent alternately. Notably, the optimizing speed of D and G is controlled by a hyperparameter q, which means that the generator is trained once when the discriminator is trained for q times.

III. DIAGNOSIS METHOD BASED ON THE GAN

Based on the GAN, this study proposes a novel intelligent fault diagnosis method that can effectively classify fault modes using a small set of samples. Unlike the classification- and clustering algorithm-based diagnosis methods, a GAN is a generative learning algorithm that can effectively mine the intrinsic distribution of a dataset using few samples. Furthermore, the discrimination ability of a GAN discriminator makes it possible to build an ensemble fault diagnosis model. Because a DNN is capable of approximating arbitrary nonlinear functions, it can be used to build the generator and discriminator in a GAN. The DNN of the generator is able to establish a nonlinear mapping from random noise to the generated samples, and the DNN in the discriminator can determine whether the input sample comes from the real data distribution. The proposed method includes the following 4 steps.

1) The first step is preprocessing the vibration signals collected from the rotating machinery. The preprocessing tasks include frequency-domain decomposition and normalization. Frequency-domain decomposition obtains the frequency spectra of vibration signals based on fast Fourier transform (FFT). The normalization task involves using min-max normalization to normalize all values to the range of [0, 1], where the normalization parameters are the minimum and maximum of the whole dataset, which contains samples under all health conditions.

2) The second step is training multiple GANs for all the health conditions. During adversarial training, the discriminator is trained through an unsupervised approach. The training process is stopped when the generator and the discriminator reach Nash equilibrium. A detailed training process will be described in III-A.

3) The third step is enhancing the discrimination ability of the discriminators in a semi-supervised way. Based on the training mechanism of a GAN, the discriminator cannot assess the correct samples with a probability close to 1. Thus, the discriminating ability enhancement of each discriminator can further improve the performance of the integrated diagnosis model. A detailed process of DAEM will be described in III-B.

4) Finally, the integrated fault diagnosis model is obtained by combining all the discriminators based on voting.

The remainder of Chapter III describes the adversarial training process of the GAN model, the DAEM process of the discriminator, and the integration process of the fault diagnosis model using all well-trained discriminators. It is noted that in the following description, k health conditions are used to further illustrate the training process.

A. ADVERSARIAL TRAINING OF THE GAN

Assuming that the training set is denoted as $\{x_k^{(i)}\}_{i=1}^m$, where k is the number of health conditions, $x_k^{(i)}$ is the ith frequency spectra of the health conditions k, and M is the number of training samples. The GAN model of the health conditions k is built with structurally symmetrical forms of G_k and D_k. The input dimension of G_k is the same as the dimension of the random vector, and the output dimension is the same as that of the real samples. Moreover, the input dimension of D_k is the same as that of the real samples, and the output dimension is one, indicating the probability value of the input vector coming from the real data distribution.

The noise distribution P_n should be chosen from a prior distribution, such as a uniform distribution, Gaussian distribution, or another distribution. The mini-batch denoted as $\{z^{(i)}\}_{i=1}^m$ is sampled from P_n as the input of the generator, where m is the size of the mini-batch. Then, $\{z^{(i)}\}_{i=1}^m$ is inputted into G_k to obtain the generated samples of mini-batch $\{G_k\left(z^{(i)}\right)\}_{i=1}^m$ through forward propagation. Additionally, the mini-batch denoted as $\{x_k^{(i)}\}_{i=1}^m$ is sampled from the real data distribution. Both $\{z^{(i)}\}_{i=1}^m$ and $\{x_k^{(i)}\}_{i=1}^m$ should be labeled to form the training set, where label 0 is assigned to $\{z^{(i)}\}_{i=1}^m$ and label 0 is assigned to $\{x_k^{(i)}\}_{i=1}^m$ correspondingly. The training set is grouped as $\{X; y\} = \{x_k^{(1)}, \ldots, x_k^{(m)}, G_k\left(z^{(1)}\right), \ldots, G_k\left(z^{(m)}\right); 1, \ldots, 1, 0, \ldots, 0\}$. The cross-entropy between the predicted values of D_k and the labels is used as the loss function for the training of D_k, which is shown in (4), since it can measure the difference between the distributions of two random variables.

$$L_D = -E\left[\log D(x_k) + \log\left(1 - D\left(x_f\right)\right)\right] = -\frac{1}{m}\sum_{i=1}^{m}\left[\log D\left(x_k^{(i)}\right) + \log 1 - D\left(x_f^{(i)}\right)\right] \quad (4)$$

To update the parameters in D_k, a backpropagation algorithm is utilized to calculate the gradient of the loss function. The updated values of the parameters of D_k, denoted as Θ_D^*, are obtained by implementing stochastic gradient descent, as shown in (5).

$$\Theta_D^* = \Theta_D - \nabla_{\Theta_D} L_D \tag{5}$$

Then, a complete GAN is formed by connecting G_k and D_k, and the loss function defined to train the generator is based on cross-entropy, as is that for training the discriminator. The corresponding function is denoted in (6).

$$\begin{aligned} L_G &= -E\left[\log\left(1 - D\left(G\left(z\right)\right)\right)\right] \\ &= -\frac{1}{m}\sum_{i=1}^{m}\left[\log\left(1 - D\left(G\left(z^{(i)}\right)\right)\right)\right] \end{aligned} \tag{6}$$

Similarly, the gradient of the loss function for each parameter of the DNN of G_k is calculated using the backpropagation algorithm. Then, the updated values of the parameters of G_k, denoted as Θ_G^*, are obtained by implementing a stochastic gradient descent method, as shown in (7), while keeping the parameters of D_k constant.

$$\Theta_G^* = \Theta_G - \nabla_{\Theta_G} L_G \tag{7}$$

The training process discussed above is repeated until G_k and D_k reach Nash equilibrium. At the end of the adversarial training process, G_k can generate samples that are very similar to real samples, and D_k can determine whether the input samples are from the real data distribution.

B. DISCRIMINATING ABILITY ENHANCEMENT METHOD FOR THE DISCRIMINATOR

To improve the performance of the final fault diagnosis model, the trained discriminators need to be enhanced before being integrated. During the adversarial training process, the discriminators are trained with both real and generated samples in an unsupervised way. As a result, each discriminator D_k has the ability to distinguish whether the input samples are actually from the kth health condition. Because D_k and G_k from the trained GAN have reached a Nash equilibrium state, D_k tends to predict a probability value of 0.5 for samples based on the k-th health condition. For samples that are not associated with the kth health condition, D_k tends to predict a probability value as close to 0 as possible.

However, for the purpose of fault diagnosis, each discriminator D_k should output a probability value as close to 1 as possible if the input sample is associated with the kth health condition and a probability value as close to 0 as possible if the input sample is not associated with the kth health condition. Moreover, because D_k is trained with the samples for health condition k, it has never processed samples from other health conditions. Thus, to further enhance the performance of the discriminators, DAEM is proposed for training them in a supervised way using a small number of labeled true samples. Because the discriminating ability enhancement process involves combining both unsupervised and supervised training, it could be regarded as a method of semi-supervised training. The purpose of this method is to enhance the ability of discriminators to tell whether the input is associated with the corresponding health condition.

To further illustrate the process of DAEM, the enhanced discriminator corresponding to the kth health condition is denoted as D_k^*. The samples from the kth health condition are labeled positive samples (labeled as 1), and the samples from all other health conditions are labeled negative samples (labeled as 0). Assuming that the number of samples from the jth health condition used for DAEM is denoted as n_j, the negative samples can be denoted as $\left(\{x_j^{(i)}\}_{i=1}^{n_j}\right), j = 1, \ldots, N \wedge j \neq k$, and the positive samples can be denoted as $\left(\{x_k^{(i)}\}_{i=1}^{n_k}\right)$, where the subscript refers to the health condition. Furthermore, D_k^* is trained using the above positive and negative samples in a supervised way based on the stochastic gradient descent approach until the loss converges to a minimum value. A schematic diagram of the DAEM process is shown in Fig. 2. Fig. 2 illustrates the DAEM process for a single discriminator, and the other discriminators can be similarly enhanced.

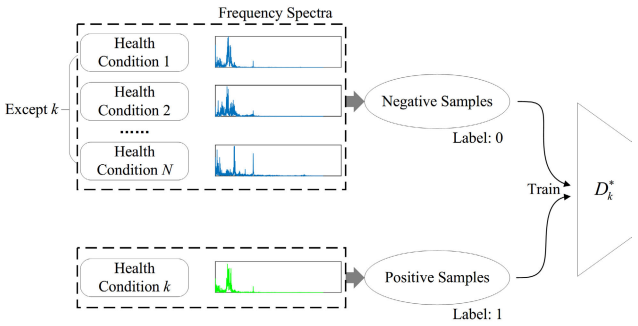

FIGURE 2. The schematic diagram of the DAEM process for D_k^*.

C. INTEGRATING THE ENHANCED DISCRIMINATORS FOR FAULT DIAGNOSIS

From the perspective of ensemble learning, the major concept involves building and training several weak classifiers and then integrating them to obtain a classifier that outperforms any one of them individually [25]. In this study, all enhanced discriminators can be regarded as weak classifiers. All the samples are pretrained in an unsupervised way using both real samples and generated samples for different health conditions, which enables them to distinguish samples associated with different health conditions. In other words, the discriminators are highly diverse in performing classification tasks, so the performance of the integrated model should theoretically surpass that of any of the weak classifiers [25].

In the proposed method, we use the voting method to predict the category of input samples. After discriminating ability enhancement, the output value of D_k^* represents the probability that an input sample is from the dataset for the kth health condition. The Softmax function is used to normalize

all the output values of the discriminators, as shown in (8).

$$Softmax\ (p)_k = \frac{\exp\left(D_k^*(x)\right)}{\sum_{i=1}^{n}\exp\left(D_i^*(x)\right)} \tag{8}$$

where $D_j^*(\cdot)$ represents the output value of the jth discriminator and $Softmax\ (p)_j$ represents the normalized probability that the input sample is associated with the jth health condition. The ensemble methodology is shown in Fig. 3.

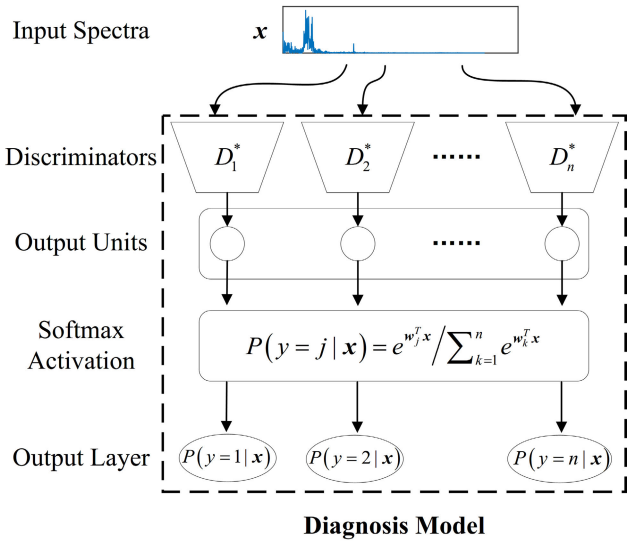

FIGURE 3. The schematic diagram of the ensemble methodology.

Additionally, the structure shown in Fig. 3 denotes the fault diagnosis process based on the proposed method. For any of the frequency spectra of a sample for a certain health condition, the integrated model predicts the classification probability value of each health condition in an end-to-end approach. Furthermore, the certain health condition corresponding to the largest probability value is the predicted category from the diagnosis model.

IV. CASE STUDY

A. CASE 1: FAULT DIAGNOSIS OF ROLLING BEARINGS

Rolling bearings are key components in rotating machinery. Severe working conditions often cause failures such as cracks, thus affecting the performance, reliability and service life of the machinery. Therefore, it is of vital importance to perform effective diagnoses of rolling bearings, provide a decision-making basis for maintenance and reduce breakdowns and economic losses. We take the diagnosis of rolling bearings as a case study to validate the performance of the proposed method.

1) DATASET DESCRIPTION

The fault data for rolling bearings used in our study were provided by Case Western Reserve University (CWRU) [26]. The data were collected from a test bench consisting of a two-hp motor, a torque transducer/encoder, a dynamometer, and control electronics, as shown in Fig. 4. The data were

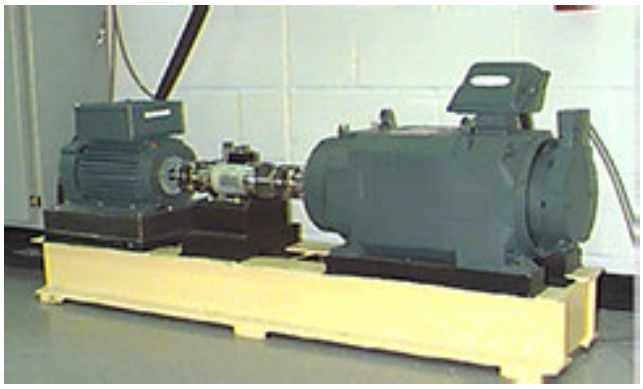

FIGURE 4. The CWRU bearing testing bench.

collected under 3 different loads (1 hp, 2 hp, and 3 hp) with a sampling frequency of 48 kHz. Four different types of fault data were collected, including normal condition (N), inner race fault (IR), rolling ball fault (B), and outer race fault (OR) data. Moreover, the fault degree was varied by using different fault diameters, including 0.007 inches, 0.014 inches, 0.021 inches, and 0.028 inches.

In this study, datasets are used to test the performance of the proposed method. Datasets A, B, and C contain vibration data collected under working loads of 1, 2 and 3 hp, where each dataset has 10 different health conditions (normal conditions and an IR, a B, or an OR fault considering different fault diameters). A detailed description of the datasets is shown in Table 1.

Because the data were collected with a sampling frequency of 48 kHz for 10 second, the vibration signal of each health condition has 480,000 points. The vibration signal of each health condition is spilt into 200 subsamples so that each subsample contains 2400 data points. Then, FFT was employed to obtain the 2400 Fourier coefficients of each subsample. Because the coefficients are symmetric, the first half of the coefficients are used in each subsample. Thus, each dataset A/B/C has 2000 samples under 10 different health conditions, and each health condition is associated with 200 samples.

2) DESCRIPTION OF THE PARAMETERS IN THE GAN

The designed generator and discriminator are structurally symmetric. The dimension of the input layer of the generator depends on the dimension of the random noise vector. The numbers of nodes in the hidden layers are 256 and 768. The output dimension of the generator is 1201, which is the same as the dimension of the spectrum samples. Correspondingly, the input dimension and the numbers of nodes in the first and second hidden layers of the discriminator are 1201, 768 and 256. The output dimension is 1 for the discriminant result. The rectified linear unit (ReLU) is employed as the activation function of the hidden layers in the generator and discriminator, and the activation functions of the output layers are sigmoid functions. To validate the performance of the proposed GAN-based method under small sample conditions,

TABLE 1. Description of the datasets.

Dataset	Working load (hp)	Number of samples	Fault type	Fault diameter (inches)	Label
A/B/C	1/2/3	200/200/200	N	/	0
		200/200/200	IR	0.007	1
		200/200/200	IR	0.014	2
		200/200/200	IR	0.021	3
		200/200/200	B	0.007	4
		200/200/200	B	0.014	5
		200/200/200	B	0.021	6
		200/200/200	OR	0.007	7
		200/200/200	OR	0.014	8
		200/200/200	OR	0.021	9

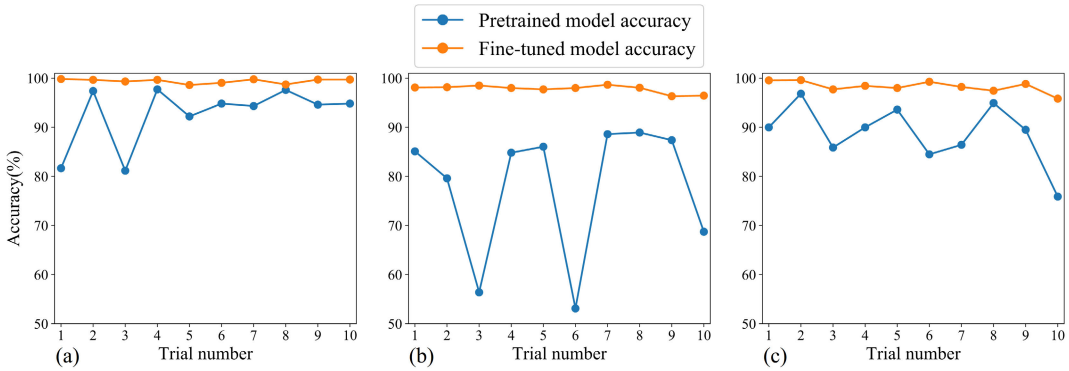

FIGURE 5. The diagnosis results of 10 independent trials using the proposed method: (a) dataset A, (b) dataset B, and (c) dataset C.

datasets A/B/C are divided into a training set and a testing set at a ratio of 1:9. Therefore, in each dataset, only 200 samples are used for training and adjusting the GAN, and the diagnosis performance is validated on 1800 unknown samples. All samples are normalized in the range of 0-1 using a min-max scaler, which takes the maximum and minimum values of the training set as the normalization parameters.

The uniform distribution was used as the prior noise distribution, and the random noise vector dimension was set to 128. The size of a mini-batch was 16. The ratio of the training times of D and G in one adversarial training epoch was 3, which means that the generator is updated once after the discriminator is updated three times. The stochastic gradient descent method was employed to update the GAN for 10000 adversarial training epochs with a learning rate of 0.01 and momentum of 0.2.

In the DAEM process of D_k^*, all 20 training samples for health condition k were selected as positive samples. To balance the numbers of positive and negative samples, 2 samples were selected from the other 9 health conditions individually as negative samples. The number of training epochs in the DAEM process was 2000. To eliminate the interference associated with other factors, ten independent experimental trials were conducted to test the performance of the proposed method.

3) EXPERIMENT RESULTS

The diagnosis results for the testing sets of datasets A, B and C using the proposed method under the parameter setting described in IV-A.2 are shown in Fig. 5. The pretrained model, which is the model after adversarial training without being enhanced, can achieve a high diagnosis accuracy for datasets A and C. As Fig. 5 shows, the diagnosis accuracy using the enhanced model is greater than 95%. A detailed description of the experimental results is given in Table. 2.

The results in Table 2 indicate that the average testing accuracy of the ten independent trials is high and the standard deviations are below 1.2%, which suggests that the proposed method is able to effectively distinguish each of the ten health conditions. It is worth noting that the high accuracy of testing is achieved under the condition that the number of training samples only accounts for 10% of all the samples. Thus, the proposed method can effectively classify different fault modes under a small sample size condition.

To further validate the performance of the proposed method under small sample conditions, experiments with different sample ratios of the training set to the test set were performed. For each dataset, the proportion of training samples to all samples was set from to 10% to 50% with an interval of 10%. Ten independent trials were conducted for each experimental setting. The experimental results shown in Fig. 6 indicate that as the size of the training set decreases, the diagnosis accuracy remains high instead of decreasing significantly. Such a result further illustrates the effectiveness of the proposed method under the condition of a small sample size.

Moreover, comparative experiments were performed under the same condition of a small sample size to illustrate the

TABLE 2. Diagnosis accuracy using the pretrained and enhanced model for datasets A/B/C, Ten trials were conducted for each dataset.

Accuracy	Dataset A		Dataset B		Dataset C	
Trial	Pretrained	Enhanced	Pretrained	Enhanced	Pretrained	Enhanced
1	81.67	99.83	85.11	98.11	90.00	99.56
2	97.39	99.67	79.61	98.17	96.83	99.61
3	81.17	99.33	56.39	98.50	85.89	97.72
4	97.72	99.67	84.83	98.00	90.00	98.44
5	92.22	98.61	86.06	97.72	93.61	98.00
6	94.83	99.06	53.11	98.00	84.50	99.28
7	94.33	99.78	88.61	98.67	86.44	98.22
8	97.61	98.72	88.94	98.06	94.94	97.44
9	94.61	99.72	87.39	96.33	89.50	98.83
10	94.83	99.72	68.72	96.44	75.89	95.83
Average	**92.64**	**99.41**	**77.88**	**97.80**	**88.76**	**98.29**
Standard deviation	6.16	0.46	13.57	0.79	6.04	1.15

TABLE 3. The experiment results for datasets A/B/C using 3 different methods.

Accuracy	The SVM-based method		The SAE-Softmax-based method		**The proposed method**	
	Average accuracy	Standard deviation	Average accuracy	Standard deviation	Average accuracy	Standard deviation
Dataset A	70.76	6.52	80.30	4.21	**99.41**	**0.46**
Dataset B	67.09	3.89	72.16	4.19	**97.80**	**0.79**
Dataset C	69.58	4.68	68.91	4.99	**98.29**	**1.15**

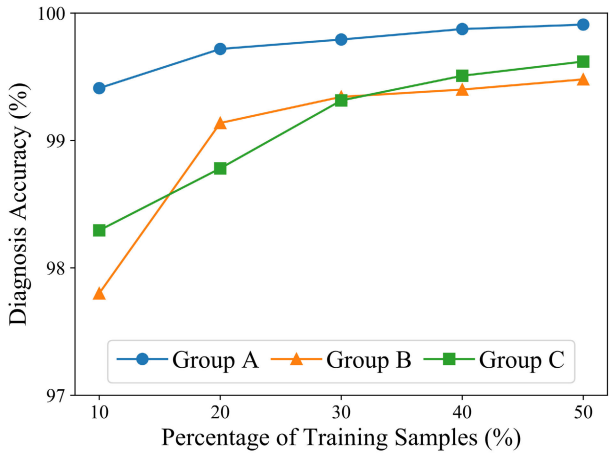

FIGURE 6. The fault diagnosis accuracy of three groups of datasets under different sizes of training sets.

effectiveness of the proposed method. The methods selected as the comparison methods were the SVM-based fault diagnosis method [5] and the stacked autoencoder (SAE)-based fault diagnosis method [13]. The percentage of training samples was selected as 10%. The configuration of the SVM-based method is obtained by a grid-search process. The penalty parameter of the error term is 1000. The SVM model uses an RBF kernel. The SAE-Softmax-based method uses an autoencoder structure containing 2 hidden layers, which has 784 and 512 neurons respectively. ReLU is chosen to be the activation function, and the optimizer is Adam. The batch-size is 32 and the model is trained for 100 epochs. The experimental results of the 3 methods are shown in Table 3.

As shown in Table 3, the proposed fault diagnosis method achieved higher accuracies and lower standard deviations than the SVM-based method and SAE-Softmax-based method. For the SVM-based method, the dimension of the inputs is too large for the traditional ML method to handle. For the SAE-Softmax-based method, the number of training samples is not sufficient for the supervised learning-based method to learn effective fault information, which makes it unable to effectively diagnose the fault modes.

4) ANALYSIS AND DISCUSSION

In this section, we first show and analyze the samples generated by the generator of the GAN. Then, the fault features extracted by the pretrained and enhanced diagnosis model are presented. Finally, the reason why the proposed method achieves good performance under small sample size conditions is discussed.

The original purpose of the GAN was to generate samples that have a similar distribution to real samples. Therefore, one key indicator of the effectiveness of adversarial training is the similarity between the generated samples and the real samples. Under the condition of using 10% of all samples in dataset A for training, the generated samples and the corresponding real samples for ten health conditions are shown in Fig. 7.

The generators are able to capture the distributions of the real samples accurately, enabling them to generate samples with high similarity to the real samples. In particular, the generators can learn the characteristic frequencies that have a critical impact on fault diagnosis, which helps to obtain a high diagnosis accuracy.

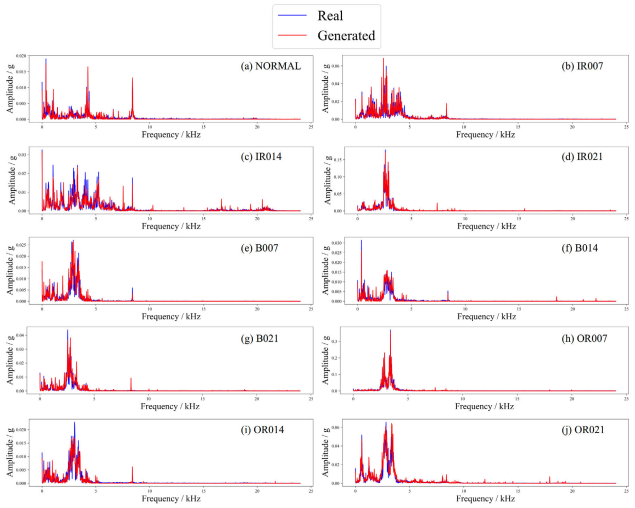

FIGURE 7. The generated samples and the corresponding real samples for (a) NORMAL, (b) IR007, (c) IR014, (d) IR021, (e) B007, (f) B014, (g) B021, (h) OR007, (i) OR014, and (j) OR021 in dataset A.

Based on the structure of the GANs introduced in section II, the discriminator receives a 1201-dimensional spectra vector as the input and extracts a 256-dimensional compressed feature vector before outputting the diagnosis result. To provide an intuitive understanding of the learning effect of the model, t-distributed stochastic neighbor embedding (t-SNE) was implemented for the feature vector to reduce the feature dimension to 3 for visualization. The scatter diagrams of the extracted features obtained by the enhanced discriminator corresponding to the normal health condition are displayed in Fig. 8. Notably, the feature points for the same health condition are clustered, and those for different health conditions are clearly separated. The visualization result based on t-SNE indicates that the enhanced discriminator can effectively extract the key information from the data, which enables it to effectively classify the data associated with different fault modes. Furthermore, the enhanced discriminator, which is trained for one specific health mode, can classify different fault modes, even though that it has only received one label corresponding to the current health mode and one other label covering all other fault modes. The reason for this high level of effectiveness is that the adversarial training and DAEM process forces the GAN to mine the differences among different categories of input samples

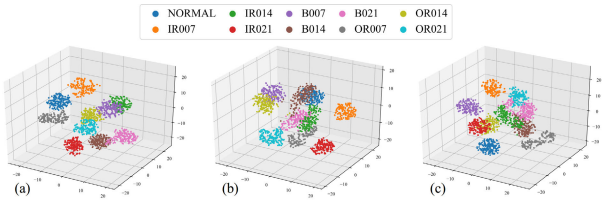

FIGURE 8. Scatter diagrams of the features extracted by the enhanced discriminator corresponding to the NORMAL health condition for (a) dataset A, (b) dataset B, and (c) dataset C.

instead of directly obtaining the label of each failure mode based on supervised learning.

As shown in Table 2 and Table 3, the proposed method can achieve an average accuracy of 99.41%, 97.80%, and 98.29% for datasets A, B, and C, respectively, under the condition of only taking 10% of all samples as the training set and performing tests based on the remaining 90% of samples. Such performance under small sample size conditions is due to the generation ability of the GAN.

During the adversarial training process, the effectiveness of the generator is gradually enhanced. Fig. 9 shows the loss trends of both the generator and discriminator during the adversarial training process and the generated samples in certain epochs. Fig. 9 shows the results obtained under normal conditions, and the ratio of the training samples to all samples is 10%. As shown in Fig. 9, the generated samples become increasingly real as the number of training epochs increases. At epoch 30, the generated samples are almost the same as the real samples, and the loss is stable regardless of the training process. Subsequently, because the generator can generate samples that are similar to the real ones, such samples can be used as augmented samples to further improve training. In Fig. 9, the generated samples obtained from epochs 30 to 100 were then used in the training process. Thus, the training set can be expanded by the generated samples. Therefore, the generating ability of the proposed method contributes to the accuracy and stability of the diagnosis.

B. CASE 2: FAULT DIAGNOSIS OF A GEARBOX

As a common transmission component, the gearbox has many advantages, such as a large transmission torque and an accurate transmission ratio. To ensure the reliability and safety of the transmission, fault diagnosis of the gearbox is necessary. In this study, to further validate the effectiveness and performance of the proposed method, another experiment was conducted using the vibration signals collected from the gearbox test bench.

1) DATASET DESCRIPTION

The test bench used to collect the data in case 2 is a power transmission fault prediction test bench manufactured by Spectra Quest, USA. It is composed of a driver (the control cabinet), a lubrication system, a driving motor, a test planetary gearbox, a test parallel gearbox, two load-parallel gearboxes, a load motor, torque sensors and force sensors. The structure of the gearbox test bench is shown in Fig. 10.

In this case, faults were injected into the planetary gear of the gearbox and included a tooth root crack, wear, one missing tooth, and a broken gear. The faulty gears corresponding to the four fault modes are shown in Fig. 11.

The rotating speed of the gears was 20 Hz, and the loads were 0 Nm (no load), 0.6 Nm, 1.2 Nm. Three different datasets, A, B, and C, were used according to different working conditions. The vibration sensor was attached to the outer end cap of the input shaft of the tested planetary gearbox via a thread connection. For each set of working

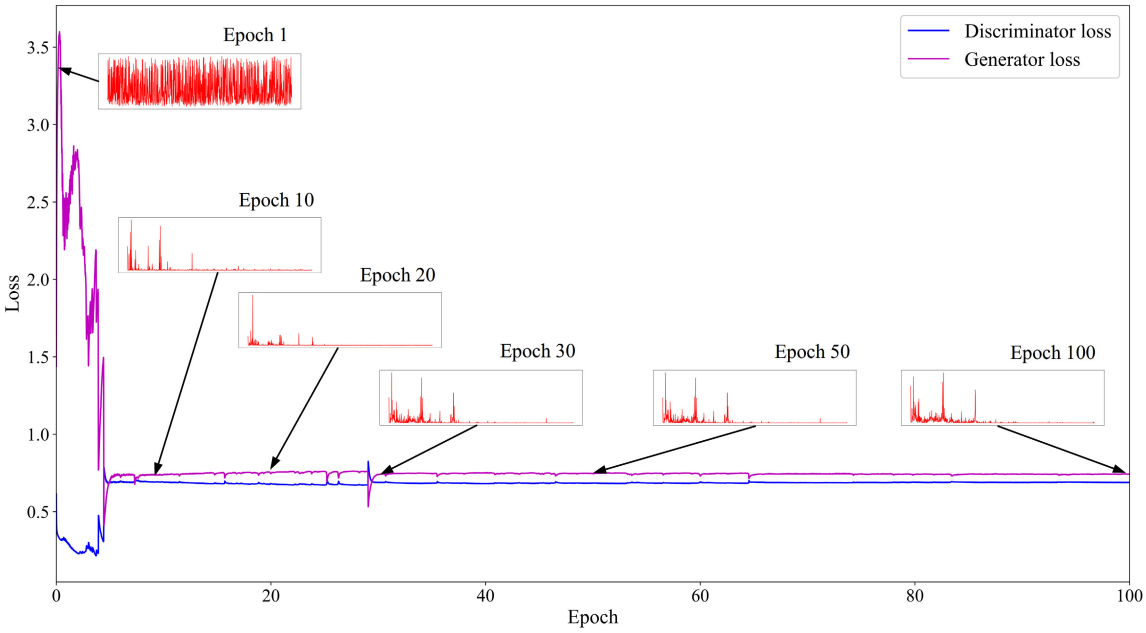

FIGURE 9. The loss trends of both the generator and discriminator during the adversarial training process.

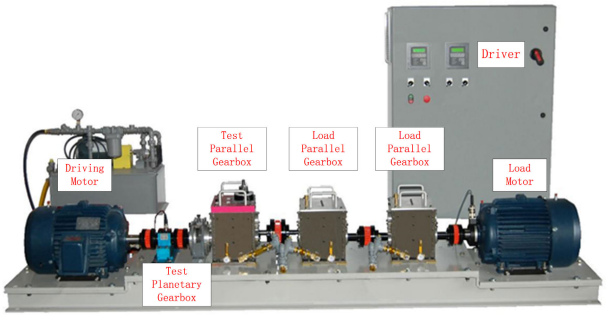

FIGURE 10. The gearbox test bench used to collect the gear fault data.

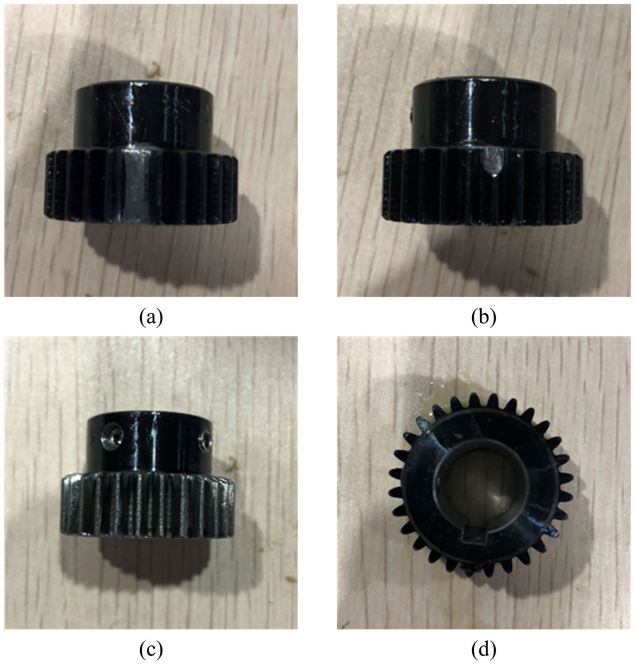

FIGURE 11. The gears corresponding to the four fault modes:(a) One missing tooth, (b) Broken, (c) Wear, and (d) Tooth root crack.

conditions, the vibration signals of the gearbox were sampled at 12.8 kHz for 40 seconds, so there were 512,000 data points for each health condition and set of working conditions. Each signal was then divided into 400 subsamples, and each subsample included 1280 data points. Furthermore, FFT was used to obtain the Fourier coefficients. Because the coefficients are symmetric, the first 641 coefficients were kept as the frequency-domain sample. Thus, each dataset included frequency-domain samples for 5 health conditions, and each health condition had 400 samples, with each sample as a 641-dimensional frequency spectrum. The details of the datasets are summarized in Table 4.

2) DESCRIPTION OF THE PARAMETERS IN THE GAN

The input dimension of the generator was equal to the dimension of the random noise vectors. The two hidden layers in the networks have 256 and 512 neurons, respectively, and the output dimension is 641, which equals the dimension of the real samples. The discriminator is symmetrical to the generator, except that the output dimension is 1, which represents the output probability value. The activation functions of the hidden layers used in the generator and discriminator are ReLUs, and the activation functions of the output layers are sigmoid functions.

Each dataset was divided into a training set and a testing set based on a ratio of 1:4. The samples in the training set

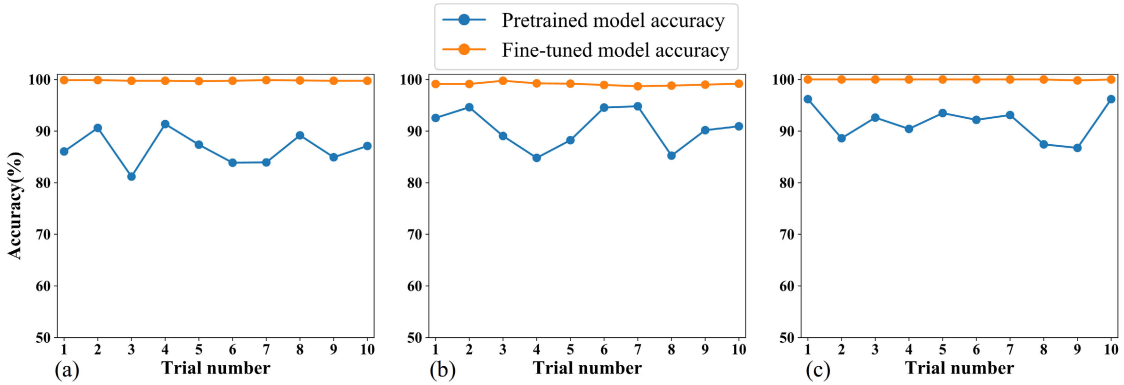

FIGURE 12. The diagnosis results of 10 independent trials using the gearbox datasets: (a) dataset A, (b) dataset B, and (c) dataset C.

TABLE 4. The details of the gearbox datasets.

Dataset	Load (Nm)	The number of samples	Health condition	Label
A/B/C	0/0.6/1.2	400/400/400	Normal	0
		400/400/400	Missing tooth	1
		400/400/400	Wear	2
		400/400/400	Broken tooth	3
		400/400/400	Root crack	4

and the testing set were normalized to the range of 0 1 using the maximum and minimum values in the training set. The random noise obeyed a uniform distribution between 0 and 1, and the dimension was 128. The size of the mini-batch used in the training process was 32. The ratio of the training times of D and G in one adversarial training epoch was 3:1. In the SGD optimizer, the learning rate was 0.01, and the momentum was 0.2. The model was trained for 10,000 epochs as part of the pretraining process of the diagnosis model. In the DAEM, the number of positive samples was the same as the number of negative samples. Using SGD as the optimizer with a learning rate of 0.01, the model was trained for 2,000 epochs. To eliminate the interference of accidental factors, 10 independent experiment trials were conducted to test the performance of the algorithm.

3) EXPERIMENT RESULTS

The accuracies of the experiments under different working loads are shown in Fig. 12. The average accuracies of the pretrained model are above 80% for the 3 different working conditions. After the DAEM process, the accuracies reach over 98%. A detailed description of the experimental results is shown in Table 5.

As shown in Table. 5, the average diagnosis accuracies of the proposed method are all above 99% for the 3 different working conditions. In particular, the accuracy of the 9 trials for dataset C is 100%, which illustrates the excellent performance of the proposed method. In addition, the low standard deviations reflect the high stability of the proposed method and indicates that the results of the different trials do not considerably fluctuate.

Comparative experiments were performed for the same conditions and a small sample size. The methods selected for comparison were the SVM-based fault diagnosis method and the SAE-Softmax-based fault diagnosis method. The ratio of training samples to all samples was selected as 20%.

TABLE 5. Diagnosis accuracy using the pretrained and enhanced models for datasets A, B, and C, Ten trials were performed for each dataset.

Accuracy	Dataset A		Dataset B		Dataset C	
Trial	Pretrained	Enhanced	Pretrained	Enhanced	Pretrained	Enhanced
1	86.06	99.88	92.56	99.13	96.19	100.00
2	90.63	99.88	94.63	99.13	88.63	100.00
3	81.19	99.75	89.06	99.75	92.63	100.00
4	91.38	99.75	84.81	99.25	90.44	100.00
5	87.38	99.69	88.25	99.19	93.50	100.00
6	83.88	99.75	94.56	98.94	92.19	100.00
7	83.94	99.88	94.81	98.69	93.13	100.00
8	89.19	99.81	85.25	98.81	93.13	100.00
9	84.94	99.75	90.19	99.00	86.75	99.81
10	87.13	99.75	90.94	99.19	96.19	100.00
Average	**86.57**	**99.41**	**90.51**	**99.11**	**91.71**	**99.98**
Standard deviation	3.22	0.07	3.71	0.29	3.34	0.06

TABLE 6. The experiment results for gearbox datasets A, B, and C using 3 different methods.

Accuracy	The SVM-based method		The SAE-Softmax-based method		**The proposed method**	
	Average accuracy	Standard deviation	Average accuracy	Standard deviation	Average accuracy	Standard deviation
Dataset A	95.44	3.86	95.14	0.54	**99.41**	**0.07**
Dataset B	77.16	27.63	74.73	1.19	**99.11**	**0.29**
Dataset C	99.61	0.30	97.64	4.53	**99.98**	**0.06**

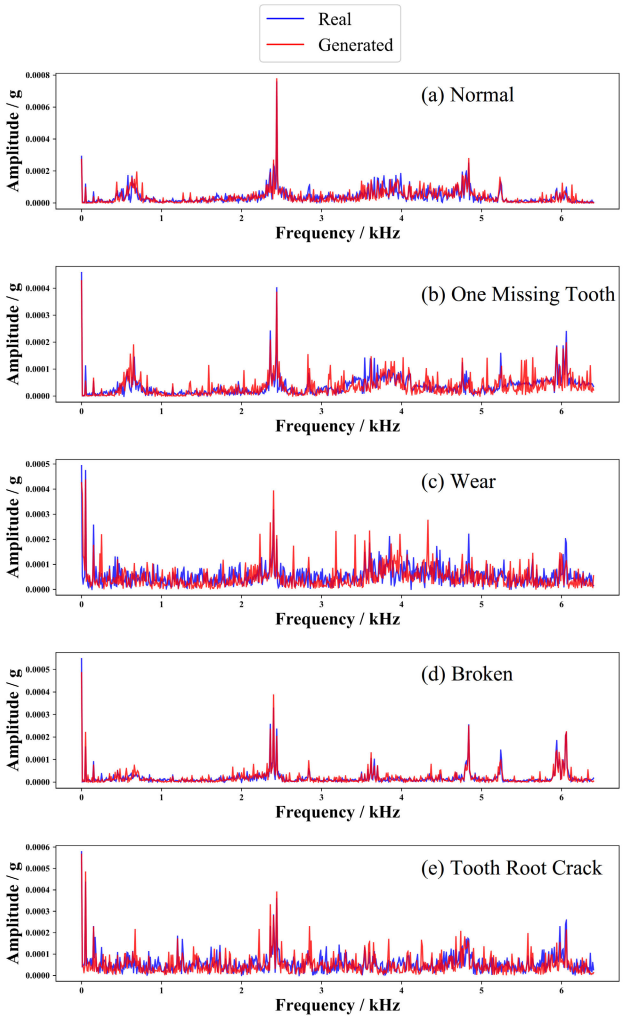

FIGURE 13. The generated samples and the corresponding real samples under (a) Normal, (b) One missing tooth, (c) Wear, (d) Broken, and (e) Tooth root crack conditions for dataset A.

The configuration of the SVM-based method is obtained by a grid-search process. The penalty parameter of the error term is 200. The SVM model uses an RBF kernel. The SAE-Softmax-based method uses an autoencoder structure containing 2 hidden layers, which has 784 and 512 neurons respectively. ReLU is chosen to be the activation function, and the optimizer is Adam. The batch-size is 32 and the model is trained for 100 epochs. The experimental results of the 3 methods are shown in Table 6.

As shown in Table 6, the proposed fault diagnosis method achieves higher accuracies and lower standard deviations than the SVM-based method and SAE-Softmax-based method.

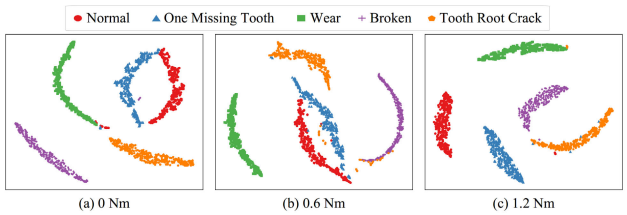

FIGURE 14. Scatter plots of the features extracted from the raw samples of different health conditions by the enhanced discriminator at (a) 0 Nm, (b) 0.6 Nm, and (c) 1.2 Nm working loads.

4) ANALYSIS AND DISCUSSION

In the case study of the diagnosis of a gearbox, we first show and analyze the samples generated by the generator in the GAN. Then, the fault features extracted by the pretrained and enhanced diagnosis model are presented. Finally, the reasons why the proposed method achieves good performance under a small sample size condition are discussed.

Taking the scenario of the gearbox under no load as an example, the comparisons between the real samples and generated samples are shown in Fig. 13. Although they are not exactly the same, the differences between the generated samples and the real samples are small, which reflects the accuracy of the generated samples. In addition, the characteristic frequencies of the generated sample and the corresponding real sample match well.

To further illustrate the effectiveness of the proposed method, the intermediate results obtained by the discriminator are visualized. Considering the structure described in section IV-B.2, the raw frequency spectrum was input into the enhanced discriminator, transformed nonlinearly by two hidden layers, and finally compressed into 128-dimensional feature vectors. We reduce the dimension of the feature vectors to 2 using principle component analysis (PCA) and t-SNE and visualize the results in the 2-dimensional plane, as shown in Fig. 14. As shown in Fig. 14, the feature points for the same health condition are clustered, and the points for different health conditions are separated. Due to the information loss of PCA, some points associated with different health conditions are mixed in 2 dimensions, but this result does not affect the diagnosis accuracy.

V. CONCLUSION

Based on a novel AI GAN, the authors proposed an intelligent diagnosis method for rotating machinery. Taking the frequency spectra of the FFT as the inputs, several GANs were trained with an adversarial approach until reaching a Nash equilibrium state. Then, the discriminator of each GAN

was detached and regarded as the pretrained weak classifier. After the discriminating ability enhancement process, all well-trained discriminators were combined into an integrated diagnosis model. When a new sample is inputted, the largest output value corresponds to the predicted health condition category. In the case studies, rolling bearings and a gearbox were investigated to validate the effectiveness of the proposed method for the fault diagnosis of rotating machinery. The high-accuracy and low-volatility results indicate that the proposed method is able to effectively extract the fault characteristics from the input signals and stably distinguish the different health conditions. In particular, we used only 10% and 20% of all samples as the training data in cases 1 and 2, respectively, and the accuracies were still above 97% for different working conditions, which indicates that the proposed method displays high performance with insufficient training data and under different working conditions. During adversarial training, the generated samples can be utilized with real samples to train the diagnosis model and can be regarded as an expansion of the training dataset to improve the generalization performance of the diagnostic model. Moreover, the training process is improved in a semi-supervised approach that provides multilabel classification ability in the model and further improves the diagnostic accuracy. Therefore, the proposed method is of vital importance in solving the problem of obtaining fault data, which are difficult to obtain in practice. In addition, because fault feature extraction is automatically completed in the proposed method, the implementation requires less prior knowledge and experience in the signal processing and fault diagnosis fields. Therefore, this method can also be applied in diagnosis tasks involving of other objects.

In the proposed method, the input feature is the spectrum of the vibration signal instead of the raw signal, thus FFT must be utilized before the training and diagnosing processes. Although the FFT requires less expert knowledge than other hand-craft feature extraction methods, signal processing still needs to be utilized and the proposed method could not be regarded as an end-to-end fault diagnosis method. In the future work, we will attempt to use the raw vibration signal to train the GANs by studying and establishing a more stable training method for GAN. Besides, we will also explore the feasibility of implementing the proposed method on other diagnosis tasks other than the rotating machinery.

REFERENCES

[1] S. J. Loutridis, "Damage detection in gear systems using empirical mode decomposition," *Eng. Struct.*, vol. 26, no. 12, pp. 1833–1841, Oct. 2004.

[2] C. Junsheng, Y. Dejie, and Y. Yu, "The application of energy operator demodulation approach based on EMD in machinery fault diagnosis," *Mech. Syst. Signal Process.*, vol. 21, no. 2, pp. 668–677, Feb. 2007.

[3] Q. Hu, Z. He, Z. Zhang, and Y. Zi, "Fault diagnosis of rotating machinery based on improved wavelet package transform and SVMs ensemble," *Mech. Syst. Signal Process.*, vol. 21, no. 2, pp. 688–705, Feb. 2007.

[4] J. Cheng, Y. Yang, and Y. Yang, "A rotating machinery fault diagnosis method based on local mean decomposition," *Digit. Signal Process.*, vol. 22, no. 2, pp. 356–366, Mar. 2012.

[5] J. Yang, Y. Zhang, and Y. Zhu, "Intelligent fault diagnosis of rolling element bearing based on SVMs and fractal dimension," *Mech. Syst. Signal Process.*, vol. 21, no. 5, pp. 2012–2024, 2007.

[6] S. Dong, D. Sun, B. Tang, Z. Gao, W. Yu, and M. Xia, "A fault diagnosis method for rotating machinery based on PCA and Morlet kernel SVM," *Math. Problems Eng.*, vol. 2014, Jul. 2014, Art. no. 293878.

[7] L.-L. Jiang, H.-K. Yin, X.-J. Li, and S.-W. Tang, "Fault diagnosis of rotating machinery based on multisensor information fusion using SVM and time-domain features," *Shock Vib.*, vol. 2014, Apr. 2014, Art. no. 418178.

[8] N. Saravanan and K. I. Ramachandran, "Incipient gear box fault diagnosis using discrete wavelet transform (DWT) for feature extraction and classification using artificial neural network (ANN)," *Expert Syst. Appl.*, vol. 37, no. 6, pp. 4168–4181, Jun. 2010.

[9] N. Saravanan, V. N. S. K. Siddabattuni, and K. I. Ramachandran, "Fault diagnosis of spur bevel gear box using artificial neural network (ANN), and proximal support vector machine (PSVM)," *Appl. Soft Comput.*, vol. 10, no. 1, pp. 344–360, Jan. 2010.

[10] A. Azadeh, M. Saberi, A. Kazem, V. Ebrahimipour, A. Nourmohammadzadeh, and Z. Saberi, "A flexible algorithm for fault diagnosis in a centrifugal pump with corrupted data and noise based on ANN and support vector machine with hyper-parameters optimization," *Appl. Soft Comput.*, vol. 13, no. 3, pp. 1478–1485, 2013.

[11] A. Krizhevsky, I. Sutskever, and G. E. Hinton, "ImageNet classification with deep convolutional neural networks," in *Advances in Neural Information Processing Systems*. New York, NY, USA: Curran Associates, 2012, pp. 1097–1105.

[12] R. Collobert and J. Weston, "A unified architecture for natural language processing: Deep neural networks with multitask learning," in *Proc. 25th Int. Conf. Mach. Learn.*, Jul. 2008, pp. 160–167.

[13] C. Lu, Z.-Y. Wang, W.-L. Qin, and J. Ma, "Fault diagnosis of rotary machinery components using a stacked denoising autoencoder-based health state identification," *Signal Process.*, vol. 130, pp. 377–388, Jan. 2017.

[14] X. Guo, L. Chen, and C. Shen, "Hierarchical adaptive deep convolution neural network and its application to bearing fault diagnosis," *Measurement*, vol. 93, pp. 490–502, Nov. 2016.

[15] L. Yu, J. Qu, F. Gao, and Y. Tian, "A novel hierarchical algorithm for bearing fault diagnosis based on stacked LSTM," *Shock Vib.*, vol. 12, pp. 1–10, Jan. 2019.

[16] Y. Hu, P. Baraldi, F. Di Maio, and E. Zio, "A systematic semi-supervised self-adaptable fault diagnostics approach in an evolving environment," *Mech. Syst. Signal Process.*, vol. 88, pp. 413–427, May 2016.

[17] L. Xu, M. Y. Chow, and L. S. Taylor, "Power distribution fault cause identification with imbalanced data using the data mining-based fuzzy classification E-algorithm," *IEEE Trans. Power Syst.*, vol. 22, no. 1, pp. 164–171, Feb. 2007.

[18] J. Yuan and X. Liu, "Semi-supervised learning and condition fusion for fault diagnosis," *Mech. Syst. Signal Process.*, vol. 38, no. 2, pp. 615–627, 2013.

[19] I. Goodfellow, J. Pouget-Abadie, M. Mirza, B. Xu, D. Warde-Farley, S. Ozair, A. Courville, and Y. Bengio, "Generative adversarial nets," in *Proc. Adv. Neural Inf. Process. Syst.* New York, NY, USA: Curran Associates, 2014, pp. 2672–2680.

[20] A. Radford, L. Metz, and S. Chintala, "Unsupervised representation learning with deep convolutional generative adversarial networks," Nov. 2015, *arXiv:1511.06434*. [Online]. Available: https://arxiv.org/abs/1511.06434

[21] A. Odena, C. Olah, and J. Shlens, "Conditional image synthesis with auxiliary classifier GANs," in *Proc. 34th Int. Conf. Mach. Learn. (PMLR)*, vol. 70, 2017, pp. 2642–2651.

[22] M. Arjovsky, S. Chintala, and L. Bottou, "Wasserstein GAN," Jan. 2017, *arXiv:1701.07875*. [Online]. Available: https://arxiv.org/abs/1701.07875

[23] Y. O. Lee, J. Jo, and J. Hwang, "Application of deep neural network and generative adversarial network to industrial maintenance: A case study of induction motor fault detection," in *Proc. IEEE Int. Conf. Big Data (Big Data)*, Dec. 2017, pp. 3248–3253.

[24] Z. Wang, J. Wang, and Y. Wang, "An intelligent diagnosis scheme based on generative adversarial learning deep neural networks and its application to planetary gearbox fault pattern recognition," *Neurocomputing*, vol. 310, pp. 213–222, Oct. 2018.

[25] S. Avidan, "Ensemble tracking," *IEEE Trans. Pattern Anal. Mach. Intell.*, vol. 29, no. 2, pp. 261–271, Feb. 2007.

[26] X. Lou and K. A. Loparo, "Bearing fault diagnosis based on wavelet transform and fuzzy inference," *Mech. Syst. Signal Process.*, vol. 18, no. 5, pp. 1077–1095, Sep. 2004.

YU DING received the B.S. degree in electronic engineering, the M.S. degree in industrial engineering, and the Ph.D. degree in systems engineering from Beihang University, China, in 2013, 2016, and 2019, respectively. His research interests include intelligent fault diagnosis and prognostics of electromechanical systems, especially deep learning, and deep reinforcement learning based methods.

LIANG MA received the B.S. degree from Beihang University, Beijing, China, in 2018, where he is currently pursuing the Ph.D. degree of systems engineering with the School of Reliability and Systems Engineering. His current research interests include fault diagnosis and prognosis, and health management based on data-driven methods.

JIAN MA received the B.S. degree in automation and the M.S. and Ph.D. degrees in systems engineering from Beihang University, China, in 2009, 2012, and 2015, respectively. He was a Visiting Scholar with Ecole Nationale SupÃl'rieure de MÃl'canique et des Microtechniques (ENSMM), France, from 2018 to 2019. He is currently an Assistant Professor with the School of Reliability and Systems Engineering, Beihang University. His current interests of research mainly include intelligent fault diagnosis and prognostics and system health management.

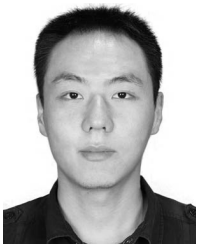

CHAO WANG received the B.Eng. degree in quality and reliability engineering and the M.A.Eng. degree in industrial engineering from the School of Reliability and Systems Engineering, Beihang University, in 2011 and 2016, respectively, where he is currently pursuing the Ph.D. degree. His research interests include machinery condition monitoring and fault diagnosis, intelligent fault diagnostics, and remaining useful life prediction.

CHEN LU was born in 1974. He received the B.Sc. degree in electronics engineering and the Ph.D. degree in power engineering from the Dalian University of Technology, China, in 1996 and 2002, respectively. From 2002 to 2007, he was a Postdoctoral Researcher with the Department of Automation, Tsinghua University, China, an Associate Professor with the Institute of Automation, China Academy of Sciences, a Postdoctoral Research Fellow with the Department of Mechanical Engineering, ParisTech-ENSAM, France, and a Visiting Scholar with the Department of Industry Engineering, University of Wisconsin, USA. Since 2007, he has been with the School of Reliability and Systems Engineering, Beihang University, China, where he is currently a Full Professor and the Executive Deputy Director of the State Key Laboratory for Reliability and Environmental Engineering. He is the author of 100 academic articles and two books, and holds more than 30 patents. His current interests of research mainly include fault detection, diagnosis, and prognostics and system health management. Prof. Lu is also the Team Leader of National Science and Technology Innovation Team, a Technical Member of Professional Board Fault Diagnosis and Safety for Technical Process of Chinese Association of Automation, and a Distinguished Professor with the Key Laboratory of Aviation Technology for Fault Diagnosis and Health Management Research. He has received many national & industrial research funds as a Principal Investigator, including the National Key Basic Research Program of China, and the National Natural Science Foundation of China. His awards and honors include the Second-Class Prize of National Science and Technology Progress Award, in 2018, the First-Class Prize of National Defense Science and Technology Progress Award, in 2017 and 2015, the Second-Class Prize of National Defense Science and Technology Progress Award, in 2013, and the Elsevier Crossley Award for Distinguished Article and Conference Best Paper Awards. He is an Associate Editor or a Guest Editor for several international journals and serves as the Chair or Co-Chair for several international conferences.